Supporting Information for

Rh nanoparticles functionalized heteroatom-doped hollow carbon sphere for efficient electrocatalytic hydrogen evolution

Defeng Qi,† Shuai Liu,† Honghui Chen,† Shuhua Lai, Yongji Qin,* Yuan Qiu, Sheng Dai,* Shusheng Zhang, Jun Luo, and Xijun Liu,*

† These authors contributed equally to this work.

Experimental section

1.1 Chemicals

Hydrofluoric acid (HF) (≥99.99998 %), tetraethyl orthosilicate (TEOS) (＞99 %), resorcinol (99 %), rhodium acetylacetonate ($Rh(acac)_3$) (99.99 %), potassium hydroxide (85 %) were obtained from Shanghai Aladdin Biochemical Technology Co., Ltd. Ethanol (EtOH) (＞99.7 %), ammonia solution (NH_3 H_2O) (25~28 %), formaldehyde (HCHO) solution (37~40 %), thiourea (≥99.5 %), hydrazine hydrate aqueous solution (N_2H_4 H_2O) (85 %) were purchased from Sinopharm Chemical Reagent Co., Ltd. Pluronic F127 (average Mn 9840-14600) was obtained from Beijing Jinming Biotechnology Co., Ltd.

1.2 Synthesis of NS-HCS

The synthesis of NS-HCS was based on a previous report with a little modification [1]. Typically, 2.8 mL TEOS was dropwise added into a mixture of 2.5 mL NH_3 H_2O, 60 mL EtOH and 20 mL H_2O for 30 min under stirring at room temperature (RT). Then 0.3 g F127 was dissolved in the above solution followed by 1.2 mmol resorcinol and 0.56 mL HCHO solution. After another 30 min stirring, 4.8 mmol thiourea and 0.42 mL HCHO solution were added. The mixture was kept stirring for 24 h at RT and then moved into a Teflon lined autoclave. The autoclave was sealed and placed in a preheated oven at 100 ℃ for 24 h. The precipitate was centrifuged, washed by H_2O and EtOH and desiccated at 60 ℃. The solid was calcined at 500 ℃ for 1 h and subsequently at 700 ℃ for 2 h with a heating rate of 1 ℃ min^{-1}. The NS-HCS was obtained after the SiO_2 core was etched by 10 wt% HF solution.

1.3 Synthesis of Rh-NS-HCS

Typically, 30 mg NS-HCS and 9 mg $Rh(acac)_3$ were dispersed in 30 mL DMF under stirring. After refluxing at 80 ℃ for 5 h, the mixture was heated at 65 ℃ to evaporate DMF. The solid was heated at 700 ℃ for 1 h with a heating rate of 5 ℃ min^{-1} and washed by 5 mL 1 M HCl at 80 ℃ for 12 h. The product was obtained after drying in oven at 60 ℃ overnight.

1.4 Characterizations

The morphology and structure were characterized by a transmission electron microscopy (TEM, FEI Talos F200X) and a scanning electron microscope (SEM, Verios 460L) operated at 20 kV. The samples for SEM analysis were sputtered before test to avoid charging. The high-angle annular dark-field scanning TEM (HAADF-STEM), energy-dispersive X-ray spectroscopy (EDX) and elemental mapping were tested by a probe-corrected TEM (PCTEM, FEI Titan Themis Cubed G2 60-300). Powder X-ray diffraction pattern (XRD) was carried out on a Rigaku SmartLab 9KW with Cu Kα radiation (λ = 1.54598 Å) at a scan rate of 10° min^{-1} from 3° to 90° operated at 40 kV and 40 mA.. The valence statuses of elements were performed on an X-ray photoelectron spectroscopy (XPS, Thermo Fisher Scientific ESCALAB 250Xi).

1.5 Electrochemical characterization

CHI 760E (Chenhua, Shanghai) workstation was utilized to measure all the electrochemical tests with a 5-necked flask for three-electrode tests and a beaker for two-electrode tests. All the inks were made by mixing 3 mg catalyst, 500 μL EtOH and 500 μL 0.5 wt% Nafion solution. After ultrasound treating for 0.5 h, 0.2 mL of inks

were dropwise dried on 1×1 cm carbon paper to make working electrodes with 0.5 mg cm^{-2} loading. In typical three-electrode system, Pt foil and Hg/HgO electrode were used as counter electrode and reference electrode, respectively. In a typical two-electrode system, two working electrodes were used as both anodic and cathodic electrodes. HER results were obtained in 1 M KOH aqueous solution, while HzOR and OHzS were carried out in the same electrolyte but with extra 0.5 M hydrazine hydrate. All potential values were transformed to reversible hydrogen electrode (RHE) potentials with IR calibration, following the equation: $E_{RHE}=E_{Hg/HgO}$ + 0.098 V + 0.059 pH. The electrochemical impedance spectroscopy (EIS) was performed from 10^5 to 10^{-2} Hz with 5 mV amplitude at open-circuit potentials.

Figures

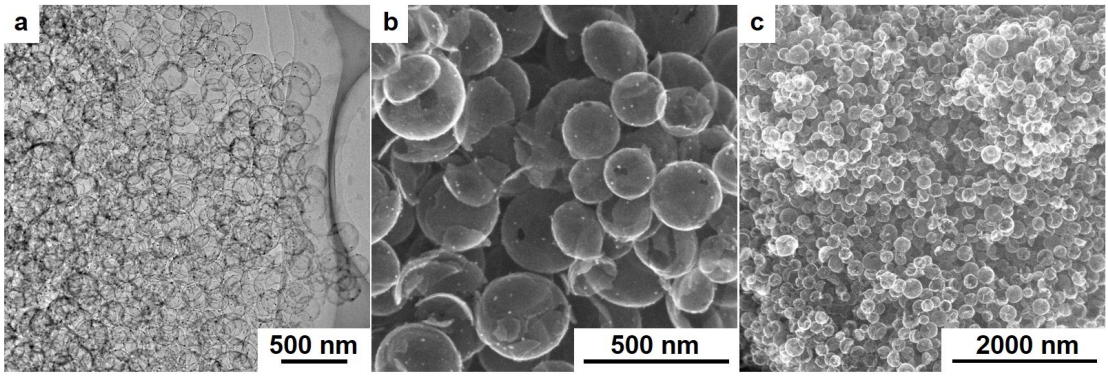

Figure S1. TEM (a), high (b) and low (c) magnification SEM images of Rh-NS-HCS.

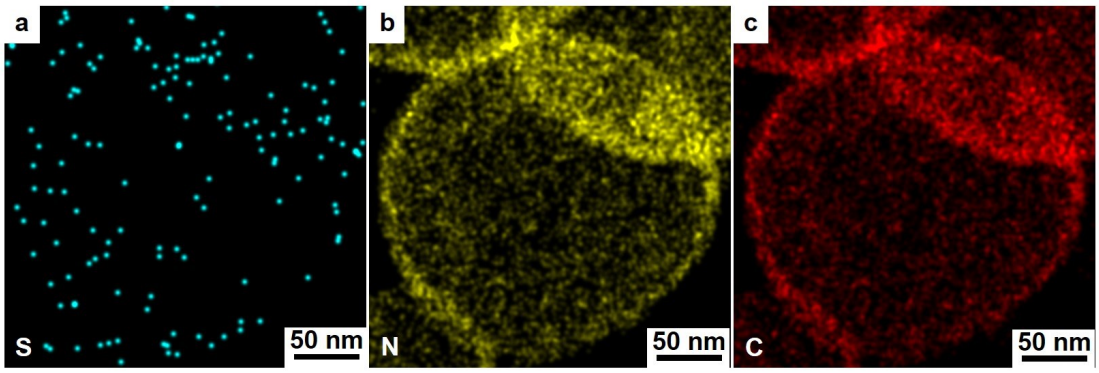

Figure S2. The elemental maps of Rh-NS-HCS : (a) S; (b) N; (c) C.

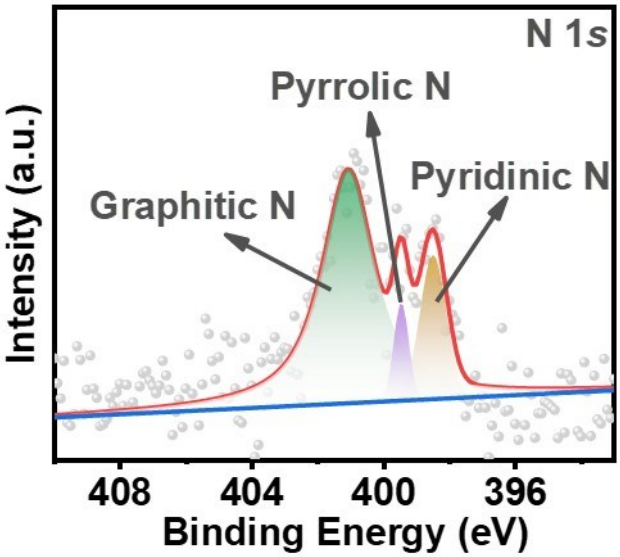

Figure S3. High resolution XPS spectra of N 1*s*. The high-resolution N 1s spectra is identified by the 401, 399.5 and 398.5 eV peaks, which could be assigned to graphitic N (77.2 %), pyrrolic N (6.4 %) and pyridinic N (16.4 %), respectively, typically observed in the case of N doping carbon materials.[2]

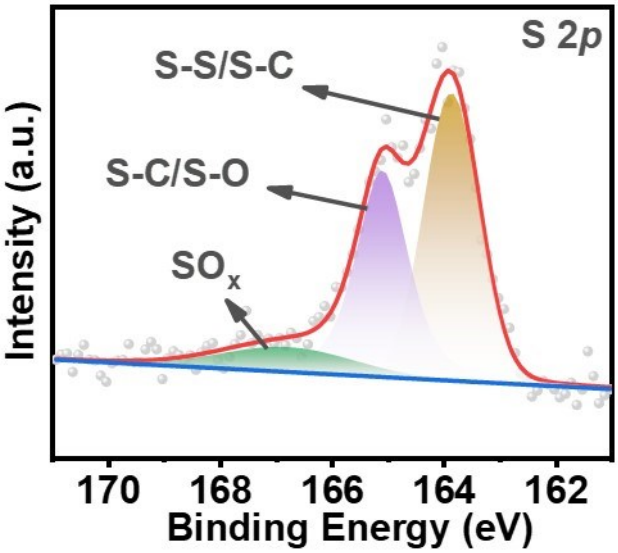

Figure S4. High resolution XPS spectra of S. The high-resolution S 2p spectra could be deconvoluted into three peaks around at 167, 165.1 and 163.8 eV, corresponding to sulfate, S-C/S-O and S-S/S-C groups, respectively.[3]

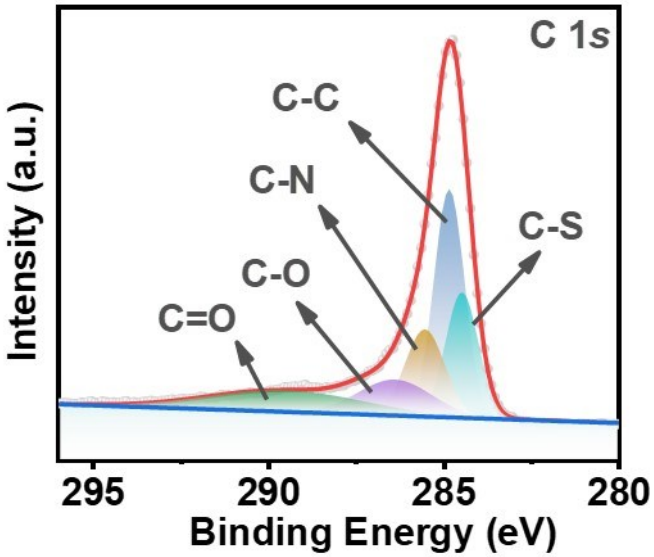

Figure S5. High resolution XPS spectra of C 1*s*.

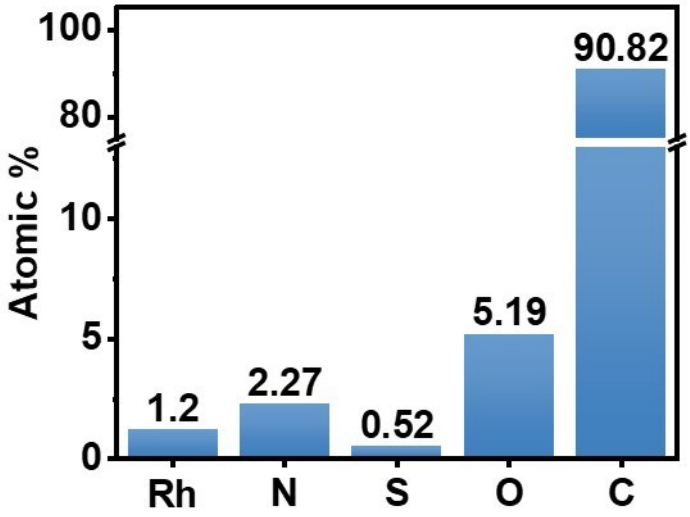

Figure S6. XPS elemental analysis of Rh-NS-HCS.

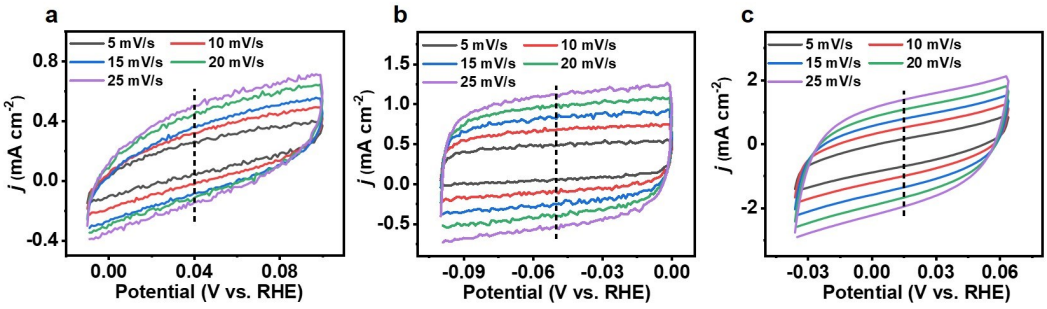

Figure S7. CV curves at different scan rates of (a) Pt/C; (b) NS-HCS; (c) Rh-NS-HCS.

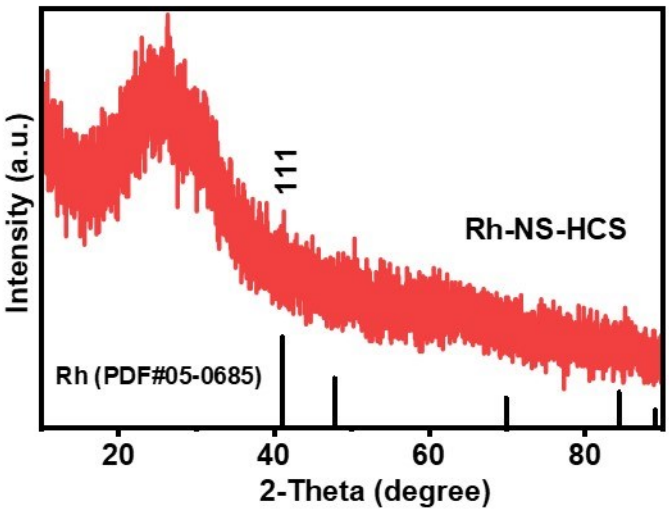

Figure S8. XRD pattern of Rh-NS-HCS after stability test.

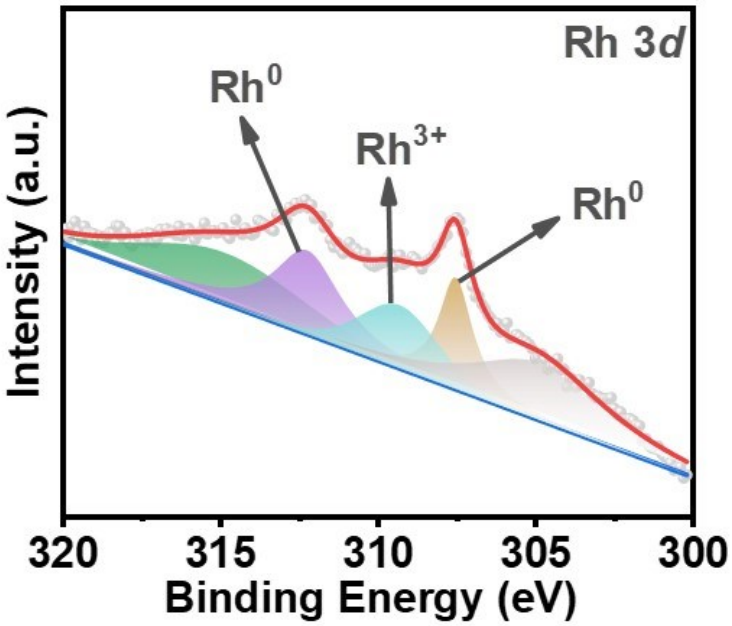

Figure S9. High resolution XPS spectra of Rh-NS-HCS after stability test.

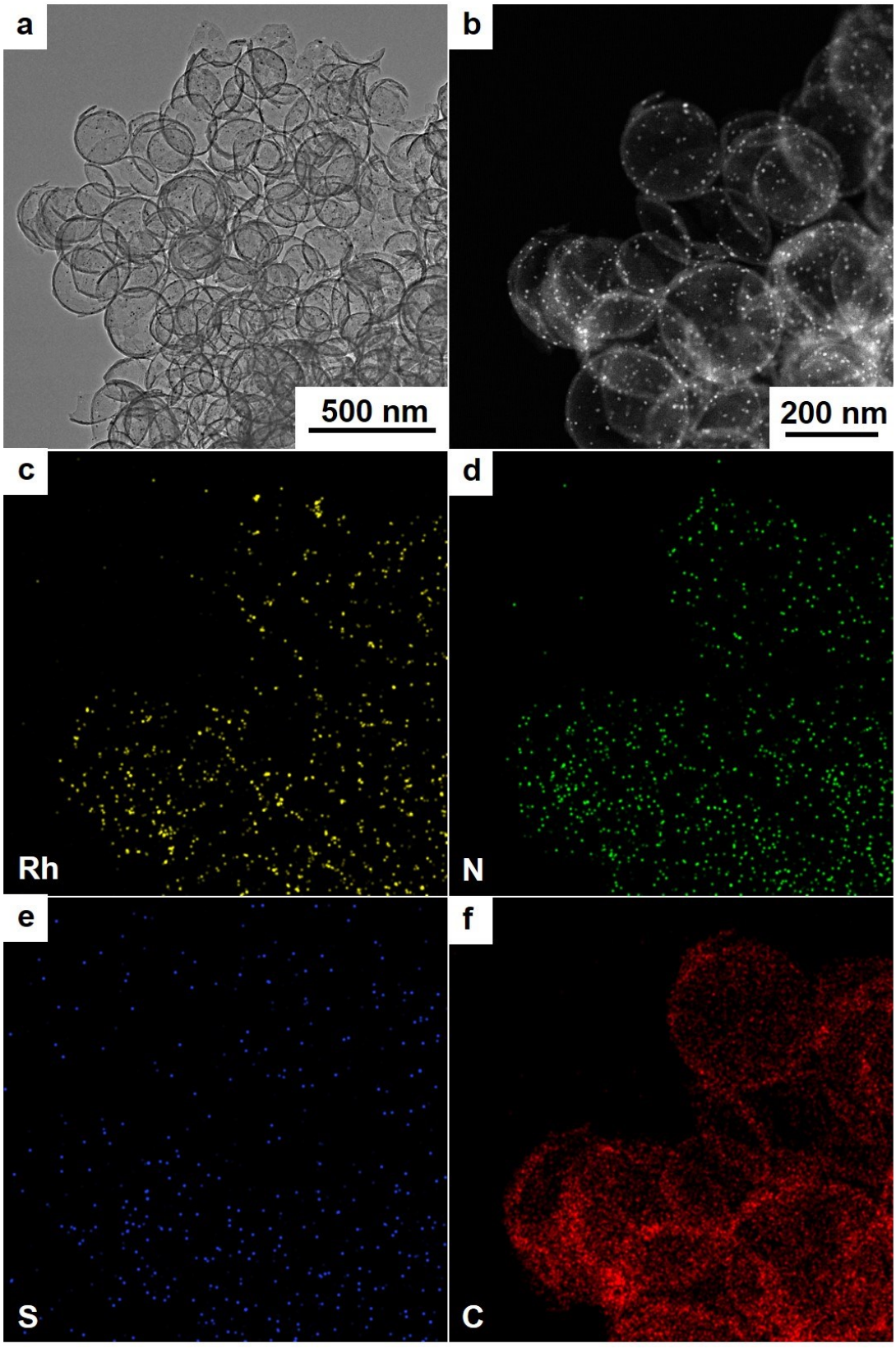

Figure S10. TEM (a), HAADF-STEM (b) and elemental mapping (c-f) images of Rh-NS-HCS after stability test.

Table S1. HER performances of this work and previous reports.

Sample	Particles size (nm)	Weight ratio (%)	Electrolyte	Overpotential at 10 mA cm^{-2} (mV)	Tafel slope (mV dec^{-1})	ref
Rh–MoSe2	2.5	8.2	1 M KOH	73	123	Inorg. Chem. Front., 2018, 5, 2978
Rh nanosheets	-	-	1 M KOH	42	30	Nanoscale, 2019, 11, 9319
Rh–Rh2O3-NPs/C	10	79.15	0.5 M KOH	63	70	J. Mater. Chem. A, 2018, 6, 23531
Rh NP/C	~ 2	23.4	1 M KOH	7	19	*Adv. Energy Mater.* 2018, *8*, 1801698
Rh/NiFeRh-LDH	0.8	4	1 M KOH	58	81.3	Nano Lett. 2020, 20, 136
0.5Rh-GS1000	3	0.5	1 M KOH	25	50	ACS Sustainable Chem. Eng. 2019, 7, 18835
Rh-doped CoFe-ZLDH	-	20	1 M KOH	28	42.8	Adv. Funct. Mater. 2020, 30, 2003556
Rh NSs	-	-	1 M KOH	43	107.2	Chem. Mater. 2017, 29, 5009
Rh_1Sn_2/SWNTs	5	-	1 M KOH	46	81.11	Int. J. Hydrogen Energ. 45 (2020) 32050
Rh@NPCP	2.5	9.84	1 M KOH	20	33	Electrochimica Acta 326 (2019) 134982
Rh-NS-HCS	4	5	1 M KOH	72	107	This work

Table S2. HzOR performances of this work and previous reports.

Sample	**Electrolyte**	**Overpotential at 10 mA cm^{-2} (mV)**	**Overpotential at 100 mA cm^{-2} (mV)**	**ref**
Cu1Nu2-N	1 M KOH + 0.5 M N_2H_4 H_2O	-	~200	*Adv. Energy Mater.* **2019**, *9,* 1900390
D-MoP/rGO	1 M KOH + 0.5 M N_2H_4 H_2O	84	-	*Inorg. Chem. Front.* **2019**, *6*, 2686
CoSe2	1 M KOH + 0.5 M N_2H_4 H_2O	-	150	*Angew. Chem. Int. Ed.* **2018**, *57,* 7649
Fe-CoS2	1 M KOH + 0.1 M N_2H_4 H_2O	-	129	*Nat. Commun.* **2018**, *9,* 4365
Ni3S2/NF	1 M KOH + 0.2 M N_2H_4 H_2O	-	415	*J. Mater. Chem. A* **2018**, *6,* 19201
Rh/N-CB	1 M KOH + 0.05 M N_2H_4 H_2O	72	-	ACS Appl. Mater. Interfaces 2019, 11, 35039
Rh2S3/NC	1 M KOH + 0.1 M N_2H_4 H_2O	95	154	Small Methods 2020, 2000208
RuP2-CPM	1 M KOH + 0.3 M N_2H_4 H_2O	70	-	*Sci. Adv.,* 2020, **6,** eabb4197
Rh2P uNSs,	0.5 M H2SO4 + 0.05 M N_2H_4 H_2O	10	-	*Applied Catalysis B: Environmental 270 (2020) 118880*
Pt(111)	0.1 M HClO4 + 1mM NaCl + 0.01 M N_2H_4 H_2O	-	450	*ChemElectroChem* **2017**, *4,* 1130
Rh-NS-HCS	1 M KOH + 0.5 M N_2H_4 H_2O	84	427	This work

Table S3. OHzS performances of this work and previous reports.

Bifunctional catalyst	**Electrolyte**	**Cell voltage @ 10 mA cm^{-2}**	**Cell voltage @ 100 mA cm^{-2}**	**ref**
CoP/TiM	1 M KOH + 0.1 M N_2H_4 H_2O	0.2 V	-	ChemElectroChem 2017, 4, 481
Ni2P/NF	1 M KOH + 0.5 M N_2H_4 H_2O	-	0.45 V	Angew. Chem. Int. Ed. 2017, 56, 842
Ni(Cu)/NF	1 M KOH + 0.5 M N_2H_4 H_2O	-	0.41 V	ACS Sustainable Chem. Eng. 2018, 6, 12746
Fe-CoS2	1 M KOH + 0.1 M N_2H_4 H_2O	-	0.95 V @ 500 mA cm-2	Nat. Commun., 2018, 9, 4365
Rh/N-CB	1 M KOH + 0.5 M N_2H_4 H_2O	0.2 V @ 20 mA cm^{-2}	-	ACS Appl. Mater. Interfaces 2019, 11, 35039
CoP/NCNT-CP	1 M KOH + 0.5 M N_2H_4 H_2O	0.89 V	-	ACS Sustainable Chem. Eng. 2019, 7, 10044
D-MoP/rGO	1 M KOH + 0.5 M N_2H_4 H_2O	-	0.74 V	:Inorg. Chem. Front., 2019, 6, 2686
PW-Co3N NWA/NF	1 M KOH + 0.1 M N_2H_4 H_2O	0.028 V	0.171 V	Nat. Commun., 2020, 11, 1853
Rh2S3/NC	1 M KOH + 0.1 M N_2H_4 H_2O	0.108 V	0.393 V	Small Methods 2020, 2000208
DHzFC	1 M KOH + 0.2 M N_2H_4 H_2O	0.071 V	0.76 V	*Angew. Chem. Int. Ed.* 10.1002/anie.202014362
Rh-NS-HCS	1 M KOH + 0.5 M N_2H_4 H_2O	0.106 V	0.595 V	This work

References

[1] S. Ma, P. Su, W. Huang, S.P. Jiang, S. Bai, J. Liu, Atomic Ni species anchored N-doped carbon hollow spheres as nanoreactors for efficient electrochemical CO_2 reduction, ChemCatChem 11 (2019) 6092-6098.
[2] T. Zhang, X. Han, H. Yang, A. Han, E. Hu, Y. Li, X.Q. Yang, L. Wang, J. Liu, B. Liu, Atomically dispersed nickel(I) on an alloy-encapsulated nitrogen-doped carbon nanotube array for high-performance electrochemical CO_2 reduction reaction, Angew. Chem. Int. Ed. 59 (2020) 12055-12061.
[3] X. Wen, X. Lu, K. Xiang, L. Xiao, H. Liao, W. Chen, W. Zhou, H. Chen, Nitrogen/sulfur co-doped ordered carbon nanoarrays for superior sulfur hosts in lithium-sulfur batteries, J. Colloid Interf. Sci. 554 (2019) 711-721.